

# Transport-mechanism analysis of the reverse leakage current in GaInN light-emitting diodes

Qifeng Shan,<sup>1</sup> David S. Meygaard,<sup>1</sup> Qi Dai,<sup>1,a)</sup> Jaehee Cho,<sup>1</sup> E. Fred Schubert,<sup>1,b)</sup> Joong Kon Son,<sup>2</sup> and Cheolsoo Sone<sup>2</sup>

<sup>1</sup>*Future Chips Constellation, Department of Physics, Applied Physics and Astronomy, and Department of Electrical, Computer, and Systems Engineering, Rensselaer Polytechnic Institute, Troy New York 12180, USA*

<sup>2</sup>*R&D Institute, Samsung LED, Suwon 443-743, Republic of Korea*

(Received 17 August 2011; accepted 21 November 2011; published online 23 December 2011)

The reverse leakage current of a GaInN light-emitting diode (LED) is analyzed by temperature dependent current–voltage measurements. At low temperature, the leakage current is attributed to variable-range-hopping conduction. At high temperature, the leakage current is explained by a thermally assisted multi-step tunneling model. The thermal activation energies (95–162 meV), extracted from the Arrhenius plot in the high-temperature range, indicate a thermally activated tunneling process. Additional room temperature capacitance–voltage measurements are performed to obtain information on the depletion width and doping concentration of the LED. © 2011 American Institute of Physics. [doi:10.1063/1.3668104]

III-V nitride based light-emitting diodes (LEDs) have attracted much attention due to their high efficiency and little adverse environmental impact. LEDs with low leakage current, including subthreshold forward leakage current and reverse leakage current, are desirable to increase the device lifetime and the electrostatic discharge resilience.<sup>1,2</sup> The reverse leakage current of GaN LEDs has been studied using temperature dependent current-voltage measurements.<sup>3</sup> It was claimed that the main conduction mechanism responsible for the reverse-bias leakage is tunneling.<sup>3</sup> In GaN *pn* junction photodetectors, the reverse leakage current was attributed to the carrier hopping through defect states in the space charge region.<sup>4</sup> The doping concentration and, accordingly, the internal electric field in the depletion region of GaN LEDs are usually much higher than in GaN photodetectors.<sup>4</sup> The transport mechanisms in GaN LEDs under reverse bias with such a high internal electric field are not fully understood. In the present article, we investigate capacitance–voltage (C–V) characteristics and temperature-dependent reverse leakage current of GaN LEDs in order to identify transport mechanisms of the reverse leakage current. At temperatures lower than 250 K, the reverse leakage current is attributed to variable-range-hopping (VRH) conduction; above room temperature, the reverse leakage current is attributed to thermally assisted multi-step tunneling.

The devices under test are  $1 \times 1 \text{ mm}^2$  GaInN LEDs with peak emission wavelength of 440 nm. The LED structure is deliberately grown for this study by metalorganic vapor phase epitaxy on *c*-plane sapphire substrate. The LED consists of an undoped GaN layer, a  $2 \mu\text{m}$  n-type GaN layer, a 15/15 nm Si-doped GaInN/GaN underlayer ( $n \sim 1 \times 10^{18} \text{ cm}^{-3}$ ), five-period undoped 3/5 nm GaInN/GaN multiple quantum wells (MQWs), a 125 nm Mg-doped AlGaIn

electron blocking layer and a Mg-doped p-type GaN layer ( $N_{\text{Mg}} \sim 8.0 \times 10^{19} \text{ cm}^{-3}$ ).

Room temperature C–V measurements are performed at a fixed frequency of 1 MHz with an AC test signal level of 15 mV. Due to the low Mg-doping efficiency in GaN-based materials and due to the high thermal activation energy of Mg acceptors, the p-type GaN is highly Mg doped. It can be assumed that the net acceptor concentration in the p-type region is much greater than the unintentional donor concentration in the MQW region.<sup>5</sup> According to the depletion approximation, the depletion region is mostly located on the lightly doped side, i.e., the MQW region and the n-type GaN region. The C–V concentration,  $N_{\text{CV}}$ , is given by<sup>6</sup>

$$N_{\text{CV}} = \frac{2}{e\epsilon_r\epsilon_0} \left[ -\frac{1}{d(1/C_{\text{UA}}^2)/dV} \right], \quad (1)$$

where  $C_{\text{UA}}$  is the measured capacitance per unit-area and  $\epsilon_r$  and  $\epsilon_0$  are the relative and absolute dielectric constants of the material, respectively. The depletion width is calculated by  $d_{\text{CV}} = \epsilon_r \epsilon_0 / C_{\text{UA}}$ . The C–V profile is the plot of  $N_{\text{CV}}$  as a function of  $d_{\text{CV}}$ . The spatial resolution of the C–V profile for quantum confined system is limited to the spatial extent of the carrier wave function.<sup>7</sup> Moreover, it was proved that the C–V concentration measured in an asymmetric *pn* junction (acceptor concentration in the p-type region  $\gg$  donor concentration in the n-type region) corresponds approximately to the free carrier concentration  $N_{\text{CV}}(z) \approx n(z)$ .<sup>6</sup> Therefore, the full width at half maximum (FWHM) of the peak in the C–V profile of a QW structure is approximately equal to the spatial width of the wave function, i.e., approximately the QW thickness. Figure 1 shows the C–V profile of the LED. In the C–V profile, there are two main, sharp peaks separated by 8.4 nm; this distance is close to the period of the MQW (8 nm). The FWHM of the second peak is 3.6 nm, which is similar to the QW thickness (3 nm) in the LED. The valley at the depletion width of 30 nm and the plateau on the right of the figure correspond to the 15 nm n-type GaN layer and 15 nm n-type GaInN

<sup>a)</sup>Present address: Bridgelux, Inc., 101 Portola Avenue, Livermore CA 94551, USA.

<sup>b)</sup>Electronic mail: efschubert@rpi.edu.

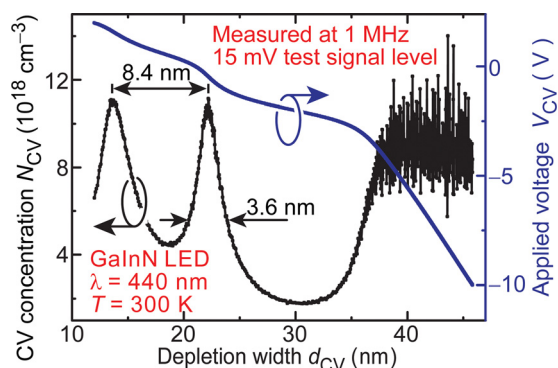


FIG. 1. (Color online) C-V profile of a GaInN LED measured at 300 K. The measurement AC test signal is at 1 MHz and the test signal level is 15 mV.

layer, respectively. The depletion width at zero bias is only about 20 nm, which indicates a strong electric field in the depletion region.

The reverse current of the LED is measured in the dark for temperatures ranging from 80 to 450 K with increments of 10 K. The LED was fabricated following the same procedure described by Kim *et al.*<sup>8</sup> The sidewall of the LED is electrically passivated with a dielectric material before the metal deposition. Thus, we assume that the sidewall surface leakage current can be neglected. In GaN based LEDs, due to the wide bandgap of GaN, the drift-diffusion current and Sah-Noyce-Shockley generation-recombination current under reverse bias are too small to be measured. Therefore, there must be other mechanisms that are responsible for the high leakage current. To investigate the leakage current mechanisms, the reverse current is measured as a function of temperature at a bias of  $-5$  V, which is shown in the Arrhenius plot of Fig. 2. At a given temperature, the derivative  $-d(\ln I)/d(kT)^{-1}$ , which is proportional to the slope in the Arrhenius plot, may be called the thermal activation energy of the conduction process. Inspection of the plot reveals that the “thermal activation energy” decreases with decreasing temperature. The low-temperature-leakage current of a GaN Schottky diode was explained by tunneling from the metal to the n-type GaN.<sup>9</sup> In GaN *pn* junctions, such as GaN LEDs,

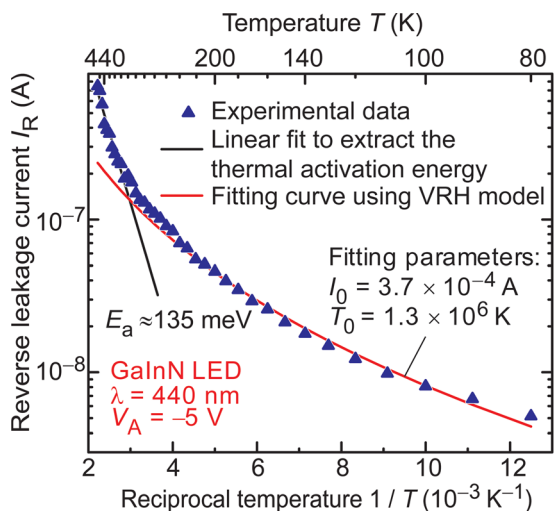


FIG. 2. (Color online) Arrhenius plot of the reverse leakage current at  $-5$  V of a GaInN LED. A VRH conduction model is used to fit the experimental data in the range of 80–250 K. The thermal activation energy is extracted from data in the temperature range 300–450 K.

the low temperature leakage is not due to the interband tunneling because of the much larger tunneling barrier. Moreover, the tunneling current does not depend on temperature. However, in our measurement, the leakage current still depends on temperature. This temperature dependence can be explained by variable-range-hopping (VRH) conduction. According to Mott’s theory,<sup>10</sup> the VRH conductivity of disordered materials, e.g., amorphous germanium, follows  $\sigma(T) \propto \exp[-(T_0/T)^{1/4}]$ , where  $T_0$  is the characteristic temperature. VRH conduction was used to explain the low temperature conductivity in semi-insulating GaN.<sup>11</sup> At low temperature, the dominant hopping conduction in a semi-insulating GaN is due to electrons hopping from one deep center to another deep center, both of which are close to the Fermi level.<sup>11</sup> In a GaN based *pn* junction, under reverse bias, the depletion region can be considered as an insulating layer with a strong electric field. Considering electric-field-enhanced hopping conduction, the current follows<sup>12</sup>  $I = I_0 \exp[-C(T_0/T)^{1/4}](1 - C'F^2/T^{1/2})$ , where  $C$  and  $C'$  are constants and  $F$  is the electric field. The temperature dependence of the field term (in a limited temperature range) is small. Therefore, at a fixed voltage, the reverse current follows Mott’s  $T^{-1/4}$  law. The defect density in GaN epitaxial layers can be high. Electrons in the valence band of p-type GaN tunnel to the deep centers, hop through deep centers in the depletion region, and finally tunnel to the conduction band of n-type GaN. As shown in Fig. 2, we apply the VRH model to fit the experimental data. It is found that this model can fit the data very well in the temperature range from 80 to 250 K. The very good fit reveals a VRH conduction with a characteristic temperature  $T_0 = 1.3 \times 10^6$  K, which is a reasonable value according to Ref. 11.

The Mott’s  $T^{-1/4}$  law does not fit the data well at temperatures above 250 K. It is found that in the high temperature range (above the room temperature), the leakage current exponentially increases with decreasing of  $1/T$ , which was also observed by Fedison *et al.*<sup>13</sup> A linear fit in the Arrhenius plot of Fig. 2 in the high temperature range yields activation energy of about 135 meV, which is much smaller than the bandgap energy of GaN. This supports the hypothesis that the (1) drift-diffusion and the (2) Sah-Noyce-Shockley generation-recombination current in the depletion region are not the main mechanisms causing the reverse leakage current, since the activation energies for these two mechanisms are on the order of the bandgap energy (much larger than what we measure).<sup>14</sup> The thermal activation energy ( $\sim 135$  meV) is attributed to the thermal excitation of the electrons through deep centers or from deep centers to the conduction band in the reverse-bias depletion region (or the corresponding process in the valence band<sup>13</sup>). The leakage current in the high temperature range can be explained by the thermally assisted multi-step tunneling. In this model, electrons transition from the valence band of p-type GaN to the conduction band of n-type GaN by multi-step tunneling and thermal activation. Figure 3 shows the schematic diagram of the hopping conduction at low temperature and the thermally assisted multi-step tunneling at high temperature. The deep centers enabling the reverse leakage current could be due to diffused Mg,<sup>15</sup> dangling bonds,<sup>4</sup> or Ga-Ga bonds occurring at dislocations.<sup>16</sup>

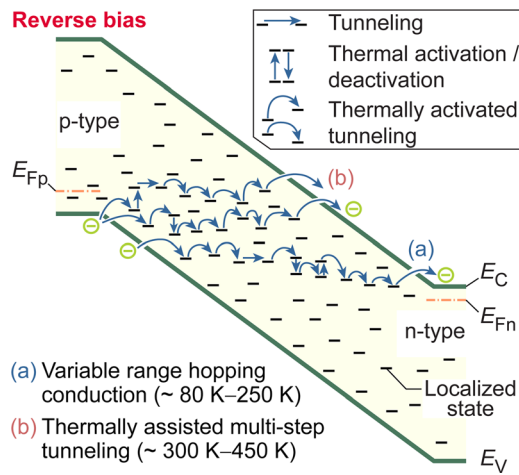


FIG. 3. (Color online) Schematic diagram of hopping conduction and thermally assisted multi-step tunneling.

The thermal activation of electrons from deep centers can be enhanced by the electric field. The lowering of the Coulombic potential barrier, due to the electric field, is the so-called Poole-Frenkel effect or field-assisted thermal ionization.<sup>17</sup> The inset of Fig. 4 shows the schematic diagram of a defect center affected by the Poole-Frenkel effect. From the Arrhenius plots, we obtain thermal activation energies in the range of 300–450 K under different bias conditions. The average internal electric field, for an applied voltage  $V_A$ , can be estimated by  $F_{AVE} = (V_{BI} - V_A)/d_{CV}$ , where  $V_{BI}$  is the built-in voltage of the GaInN LED (assumed to be 3.4 V), and  $d_{CV}$  is the depletion width obtained from the C–V measurement. The thermal activation energies are then plotted as a function of the square root of the average internal electric field, as shown in Fig. 4. According to Poole-Frenkel theory, the barrier lowering of a deep center can be expressed as  $\Delta E_a = \beta_{PF} F^{1/2} = (e^3/\pi \epsilon_0 \epsilon_r)^{1/2} F^{1/2}$ , where  $\beta_{PF}$  is the Poole-Frenkel coefficient. The calculated Poole-Frenkel coefficient of GaN material is  $\beta_{PF} = 1.2 \times 10^{-23} \text{ C(Vm)}^{1/2}$ , while the linear fit of the data in Fig. 4 yields a Poole-Frenkel coefficient of  $2.8 \times 10^{-23} \text{ C(Vm)}^{1/2}$ ; this is very close to the calculated value.

In summary, the C–V measurements and temperature dependent I–V measurements on a GaInN LED are analyzed. Quantum wells in the MQW region are well resolved as shown by two peaks in the C–V profile. The small depletion width indicates a very strong internal electric field in the depletion region. The reverse leakage current of the GaInN LED at  $-5 \text{ V}$  is plotted in an Arrhenius plot. At low temperatures (80–250 K), the carrier transport is attributed to the VRH conduction. At high temperatures (300–450 K), the thermal activation energies (95–162 meV) extracted from the Arrhenius plot are attributed to the thermal activation of electrons. The associated leakage current occurs through thermally assisted multi-step tunneling.

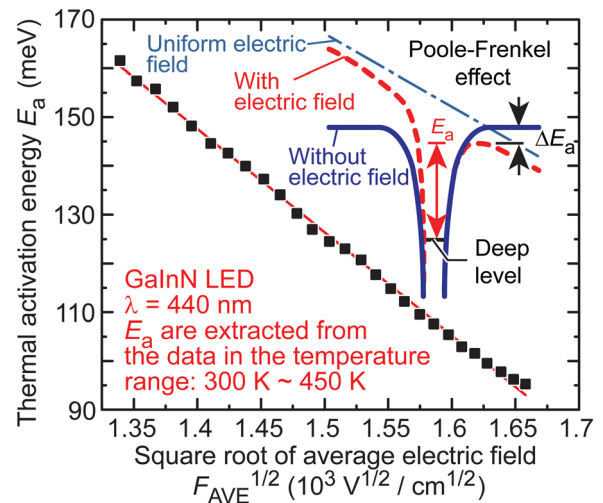


FIG. 4. (Color online) Thermal activation energy as a function of the square root of the average internal electric field in the depletion region for a GaInN LED; the inset shows the schematic diagram of the Poole-Frenkel effect.

The authors gratefully thank Samsung LED, National Science Foundation, New York State, Sandia National Laboratory, Department of Energy, Korean Ministry of Knowledge Economy and Korea Institute for Advancement of Technology through the International Collaborative R&D Program, Magnolia Optical Technologies, and Raydex Technology, Inc.

- <sup>1</sup>J. Cho, A. Mao, J. K. Kim, J. K. Son, Y. Park, and E. F. Schubert, *Electron. Lett.* **46**, 156 (2010).
- <sup>2</sup>X. A. Cao, P. M. Sandvik, S. F. LeBoeuf, and S. D. Arthur, *Microelectron. Reliab.* **43**, 1987 (2003).
- <sup>3</sup>X. A. Cao, J. A. Teetsov, F. Shahedipour-Sandvik, and S. D. Arthur, *J. Cryst. Growth* **264**, 172 (2004).
- <sup>4</sup>D. V. Kuskonov, H. Temkin, A. Osinsky, R. Gaska, and M. A. Khan, *Appl. Phys. Lett.* **72**, 1366 (1998).
- <sup>5</sup>N. C. Chen, W. C. Lien, Y. S. Wang, and H. H. Liu, *IEEE Trans. Electron. Devices* **54**, 3223 (2007).
- <sup>6</sup>E. F. Schubert, *Doping in III-V Semiconductors* (Cambridge University Press, Cambridge, 1993).
- <sup>7</sup>E. F. Schubert, R. F. Kopf, J. M. Kuo, H. S. Luftman, and P. A. Garbinksi, *Appl. Phys. Lett.* **57**, 497 (1990).
- <sup>8</sup>H. Kim, J. Cho, Y. Park, and T.-Y. Seong, *Appl. Phys. Lett.* **92**, 092115 (2008).
- <sup>9</sup>E. J. Miller, E. T. Yu, P. Waltereit, and J. S. Speck, *Appl. Phys. Lett.* **84**, 535 (2004).
- <sup>10</sup>N. F. Mott, *Philos. Mag.* **19**, 835 (1969).
- <sup>11</sup>D. C. Look, D. C. Reynolds, W. Kim, Ö. Aktasm, A. Botchkarev, A. Salvador, and H. Morkoç, *J. Appl. Phys.* **80**, 2960 (1996).
- <sup>12</sup>R. M. Hill, *Philos. Mag.* **24**, 1307 (1974).
- <sup>13</sup>J. B. Fedison, T. P. Chow, H. Lu, and I. B. Bhat, *Appl. Phys. Lett.* **72**, 2841 (1998).
- <sup>14</sup>S. M. Sze and K. K. Ng, *Physics of Semiconductor Devices*, 3rd ed. (John Wiley & Sons, Inc., Hoboken, 2007).
- <sup>15</sup>A. Mao, J. Cho, Q. Dai, E. F. Schubert, J. K. Son, and Y. Park, *Appl. Phys. Lett.* **98**, 023503 (2011).
- <sup>16</sup>L. Lymparakis, J. Neugebauer, M. Albrecht, T. Remmele, and H. P. Strunk, *Phys. Rev. Lett.* **93**, 196401 (2004).
- <sup>17</sup>J. Frenkel, *Phys. Rev.* **54**, 647 (1938).